CrossMark

ORIGINAL ARTICLE

Enhanced removal of dissolved aniline from water under combined system of nano zero-valent iron and *Pseudomonas putida*

Raj Shekhar Bose[1] · Sayan Dey[2] · Saswati Saha[2] · Chandan Kr. Ghosh[2] · Mahua Ghosh Chaudhuri[2]

Abstract Aniline is a toxic chemical released by many industries. Removal of pollutants by micro-organisms is the most recent area of research whereas nano zero valent iron (nZVI) in recent time has been widely used in treatment of groundwater. The present study aims to understand the nature of interaction of nZVI with bacteria and removal of aniline under a combined system of bacteria and nZVI. nZVI were synthesized through conventional process and its adsorption studies on aniline removal were performed. *Pseudomonas putida* MTCC 1194 strain was acclimatized to aniline in Basal salt medium for a period of 2 months. The maximum growth rate and yield coefficient of cells were determined and within 6 h 99 % removal of 200 ppm aniline was found to be achieved. Adsorption studies were performed using nZVI of different concentration on 200 ppm aniline for 6 h. Maximum aniline removal was obtained at 85 % in distilled water and 92 % in basal salt medium, respectively using 5 g/L nZVI. nZVI was found to be growth inducer to the mentioned strain. A combined system of aniline removal was studied consisting of biodegradation and adsorption to nZVI in which 99 % aniline removal was obtained in 2.5 h containing 61 % of aniline removal through biodegradation and the rest through collective adsorption and biosorption. Maximum adsorption to nZVI was found during the lag phase of cell growth and on reaching log phase adsorption rate declined and removal through biodegradation dominated.

Keywords *Pseudomonas putida* · Aniline · Adsorption · Biodegradation · nZVI · Growth promoter · Combined removal

Introduction

Aniline is a toxic chemical present in the effluent of many industries as it is widely used as a raw material in the manufacturing of a number of products such as dyes, plastics, resins, pharmaceuticals, petro-chemicals, herbicides, pesticides among others (US EPA 1985). Its other source is through natural microbial transformation of several nitro aromatic compounds (Hallas and Alexander 1983; Kinouchi and Ohnishi 1983). Aniline is a major breakdown product of diphenylamine and p-aminoazobenzene (Zissi et al. 1997).

On being released into the environment through wastewater it gets adsorbed to organic matter and gets easily transported into aquatic ecosystems and by leaching through the soil it often reaches the aquifer (Howard 1989; US EPA 1985). Maximum concentration of 36 ppb has been measured in an aquifer near underground coal gasification site in Wyoming (Howard 1989). Aniline has been found to be highly toxic to aquatic life with reported acute LC_{50} values for daphnids are less than 1 mg/L whereas chronic values are less than 0.1 mg/L (Rabert 1991). According to EPA aniline has also been found to possess genotoxicity, neurotoxicity and reproductive toxicity in human and animals. EPA has also listed aniline in B2

✉ Mahua Ghosh Chaudhuri
mahua_ch@yahoo.com

[1] School of Environmental Studies, Jadavpur University, Kolkata 700032, India

[2] School of Materials Science and Nanotechnology, Jadavpur University, Kolkata 700032, India

 Springer

category, probable human carcinogen (US EPA 1985; Beard and Noe 1981).

Many bacterial community in the soil, for example, *Pseudomonas* sp, Acinetobactersp, Rhodococcussp, etc. have been shown to degrade aniline completely through bioremediation by using it as their sole carbon source (Ang et al. 2009; Donald 2000; Wasi et al. 2013). Anilines are metabolized to the corresponding catechols via one or more oxidative reactions catalyzed by aniline dioxygenases, liberating ammonia and subsequently undergoing metabolic transformations (Loidl et al. 1990; Fuchs et al. 1991).

In recent times nano zero valent iron (nZVI) has been used extensively in treatment of groundwater owing to possessing of excellent chemical and surface property. nZVI possesses excellent reducing property which causes dehalogenation reaction in groundwater contaminated with toxic halogenated hydrocarbon like Poly-chlorinated biphenyls and perchloro ethylene, etc. and converts them into non-toxic forms (Patil and Shinde 1988; Elliott and Zhang 2001; Mueller et al. 2012). nZVI also possesses excellent adsorptive property owing to its high surface to volume ratio which has been exploited in adsorbing various heavy metal ions like Cu^{2+}, Zn^{2+}, Cd^{2+}, Cr^{6+}, Hg^{2+}, As^{3+}, etc. (Zhang 2003; Qiu et al. 2013; Lin et al. 2008; Li et al. 2010; Madhavi et al. 2013; Prabu et al. 2016; Liang et al. 2014; Yuan and Lien 2006; Vernon and Bonzongo 2014). And also many organic compounds like phenol and 4-chloro-2-nitrophenol have been shown to get removed by adsorption onto nZVI (Boparai et al. 2011; Shimizu et al. 2012; Adami and Fakhri 2013). The mechanism involves under aerobic conditions a shell of FeO(OH) layer is formed on nZVI surface which increases the affinity for adsorption (Buddhika et al. 2011; Greenlee et al. 2012; Eagleson 1994).

Many researches have suggested toxic nature of nZVI to bacterial communities under anaerobic conditions (Martin et al. 2008; Kim et al. 2011; Honghai et al. 2008; Nassar and Ringsred 2012). But in presence of oxygen an outer shell of FeO(OH) layer have been reported to be formed on nZVI surface and due to the formation of the outer shell layer of FeO(OH) bacterial growth promotion and biofilm generation have been reported in case of several bacterial community (Otte et al. 2013; Jang et al. 2014; Yang et al. 2013).

Most of the adsorbents used in industrial wastewater treatments like Granular Activated Carbon (GAC) have no positive impact on the microbial community (Fiore and Babineau 1977) moreover generation of GACs leave high quantity of environmental carbon footprints (He 2012). In contrast nZVI have been reported to possess good adsorptive property due to the presence of large number of unsatisfied dangling bonds on the surface. As the size of the nZVI is in the nanometric range, the surface to volume ratio is increased drastically thereby increasing the number of active adsorption (oxygen rich) sites are formed (Li et al. 2010; Yuan and Lien 2006; Vernon and Bonzongo 2014). Moreover, it has growth promoting impact on bacterial communities and its synthesis also have been shown to take place in room temperature (Zhao et al. 2011). Thus, it is possible to use nZVI as a dual purpose material aiding to both adsorption of organic pollutants (presence of adsorption sites) and microbial growth promoter (biofilm generation) that enhances bacterial growth which in also aids in removal of organic toxic pollutants from water. Such kind of combined system involving both biodegradation and adsorption have not been studied or reported yet in scientific literatures. Thus the present work was intended to study the removal of dissolved aniline from water using previously reported phenol and cresol degrading bacteria *P. putida* MTCC 1194 strain (Kumar et al. 2005), in the presence of nZVI particles.

In this paper, we aim to prepare an environment friendly waste water remediation system based on nZVI where the nanoparticles are used both as an adsorbent as well as a growth promoter to perform enhanced removal of Aniline from industrial waste water. We also try to ensure complete collection of the adsorbent from the treated water to prevent any elemental foot printing which is not possible for conventional carbon purification systems due to their non-magnetic nature.

Materials and methods

Chemicals

All the chemical used for synthesis of zero valent nano iron (nZVI), preparation of Basal salt medium and culturing of cell are as follows: ferric chloride (99 % pure), sodium borohydride (99 % pure), carboxy-methylcellulose (CMC) (99 % pure), K_2HPO_4 (99 % pure), KH_2PO_4 (99 % pure), $(NH_4)_3PO_4$ (99 % pure), NaCl (99 % pure), Na_2SO_4 (99 % pure), $FeSO_4 \cdot 7H_2O$ (99 % pure), $CaCl_2.2H_2O$ (99 % pure) and D-glucose (99 % pure) were purchased from MERCK India Pvt Limited, Nutrient broth and nutrient agar was purchased from Himedia. All chemicals were used without further purification.

Microorganism

The bacterial strain *P. putida* (MTCC 1194) was procured from Microbial Type Culture Collection and Gene Bank (MTCC) Chandigarh in freeze dried form. The strain was first revived in nutrient broth medium cultured overnight at 150 rpm shaking and 25 °C incubation and pH adjusted to 7 ± 0.1. From the nutrient broth medium a loop full of

strain was transferred into nutrient agar slant in culture tubes for storage.

Synthesis and characterization of nZVI

nZVI was prepared using the method described by Zhao et al. (2011); from reduction of Iron(III) chloride in nitrogen environment using Sodium borohydride and capping them using water soluble capping agent Carboxymethyl cellulose (CMC).

The properties of prepared CMC capped nZVI were investigated using Ultima-III, Rigaku X-ray diffractometer (XRD, Cu K_α radiation, $\lambda = 1.5404$ Å, scan range 10°–80°, 0.2 deg/min), Field emission scanning electron microscope (FESEM, S-4800, Hitachi) and Transmission electron microscope (TEM, JEOL) with voltage 220 kV.Shimadzu IR Prestige-21 FTIR spectrometer was used to identify the capping of nZVI with CMC.

Aniline adsorption onto nZVI in distilled water

The aniline adsorption experiment was performed following the reported method previously used (Yang et al. 2008; Al-Johani and Salam 2011; Zhao et al. 2011). Keeping the concentration of aniline (adsorbate) fixed at 100 ppm, 1 g/L of nZVI (adsorbent) was added in series of 250 mL volume of Erlenmeyer flasks containing 100 mL of 100 ppm aniline solution. Experiment was carried out inside BOD incubator with constant temperature set at 30 °C and kept for shaking at 200 rpm for thorough dispersal of nZVI in solution. pH was maintained at of 7 ± 0.1 throughout so as to prevent any degradation arising from generation of OH radicle, since lower pH favors the formation of reactive OH radicle through Fenton's reagent (Shimizu et al. 2012; Anotai et al. 2006). Another flask containing equal concentration of aniline subjected to similar conditions but devoid of nZVI was kept as control to determine loss of aniline if any through evaporation, auto-degradation or photo-degradation. The experiment was conducted in triplet. The adsorption process was carried out for 15, 30, 45 min, 1, 1.5, 2 and 3 h to determine the effect of contact time on aniline adsorption. Each solution after their respective time intervals were centrifuged twice at 20,000 rpm for 10 min to remove any nZVI particle and the supernatant were collected in glass vials and were taken for analysis under UV–Vis spectrophotometer between range 200–250 nm wavelength considering the peak value at 232 nm to determine the concentration of aniline present in the solution after the experiment. Amount of aniline adsorbed was calculated by preparing standard calibration curve as used by Johani and Salem. UV–Vis spectral analysis of each samples for each time interval were performed similarly as described previously. After determining initial and final aniline concentrations of the solution by UV–Vis spectral analysis at each time interval, adsorption percentage was calculated as follows:

$$\text{Adsorption } \% = \frac{\text{Co}-\text{Ce}}{\text{Co}} \times 100$$

where Co $=$ initial concentration of aniline,

Ce $=$ final concentration of aniline.

After the adsorption experiment, the adsorbent left was collected and dried overnight in vacuum drier prior to performing IR and XRD studies. The result obtained was plotted in Originlab 8.0 (Deschenes and David 2000) for analysis.

After the adsorption experiment, the adsorbent left was collected and dried overnight in vacuum drier prior to performing IR and XRD studies. The results obtained were plotted in Originlab 8.0 for analysis.

Acclimatization and growth kinetics determination of *P. putida* in aniline

A loop full of strain was collected from slants prepared in culture tubes and were cultured in nutrient broth medium overnight at 200 rpm shaking and 25 °C incubation and pH adjusted to 7 ± 0.1. The entire medium was centrifuged at 8000 rpm for 10 min and cell pellets were re-suspended in basal salt medium containing 2 % D-Glucose and 10 ppm aniline. Solution of basal salt medium was prepared according to composition mention by Ullhyan and Ghosh (Ullhyan and Ghosh 2012). On transferring the cell pellets, initial turbidity in the basal salt medium was adjusted to 0.1 at OD_{600}. It is known that the bacteria consumes aniline by the process of co-metabolism, that is, cells first consumes the D-Glucose in the solution, once all the D-Glucose is consumed few cells starts feeding on aniline and thus only those cells continue to survive and reproduce which have got adapted to aniline as food source. After interval of every 24 h, aniline concentration was noted by measuring the absorbance at 232 nm using UV–Vis spectrophotometer and pH was measured using pH meter. Each time when 90 % of aniline was found to be consumed, fresh 10 ppm aniline was added into the same medium. pH was found to increase at regular interval, hence it was adjusted every time to 7 ± 0.1 using 10^{-1} N HCl and 10^{-1} N NaOH stock solution kept initially prepared. After every 10 days the concentration of aniline was increased to 20, 40, 80, 160 ppm.

1 mL of media of different OD_{600} value (0.1–0.2) were centrifuged at 8000 rpm for 10 min and dried perfectly in vacuum drier for 24 h and were weighed. Weight of dry cell mass of respective OD_{600} values were plotted to generate a calibration curve (Ghasem Najafpour 2015). From the calibration curve approximate weight of dry cell mass per turbidity value was predicted.

146

Sustain. Water Resour. Manag. (2016) 2:143–159

After an acclimatization period of 2 months the cells were sub-cultured once in nutrient broth medium overnight under same conditions mentioned previously and centrifuged at 8000 rpm for 10 min and cell pellets were resuspended in basal salt medium with cell mass concentration adjusted to 0.1 at OD_{600} with containing no D-Glucose, only aniline in concentration 10 ppm. Cell growth was studied for a period of 4 h by analyzing the rise in medium turbidity at OD_{600}. Cell growth rate (μ_g) was investigated during the log phase of growth which was obtained mostly between 1.5 and 4 h. Similarly, cell growth rate were investigated for 20 ppm, 50, 100, 200, 300, 400 and 500 ppm and maximum experimentally observable cell growth rate was found to be 0.21 h^{-1} at concentration 200 ppm. Cell growth and aniline consumption for solution containing 200 ppm aniline was analyzed for a period of 6 h.

Bacterial aniline removal kinetics study

Aniline acclimatized culture were sub-cultured once in nutrient broth for overnight and cell mass were collected via centrifugation at 8000 rpm for 5 min and were transferred into 100 mL basal salt medium solution containing 200 ppm aniline in 250 mL Erlenmeyer flask. The cell mass concentration was adjusted to 0.1 at OD_{600}, pH to 7 ± 0.1 and the experiment was performed at inside BOD incubator at constant temperature set at 30 °C with shaking speed of 200 rpm. Another flask containing equal concentration of aniline subjected to similar conditions but devoid of bacterial culture was kept as control to determine loss of aniline if any through evaporation, auto-degradation or photo-degradation. The experiment was conducted in triplet. 1 mL of solution was drawn after every 30 min in 2 mL centrifuge tubes and cell mass concentration was measured at OD_{600} under UV–Vis spectrophotometer. After measuring the cell mass concentration every time the sample were centrifuged at 8000 rpm for 5 min to separate out cell mass and the supernatant was used to determine the concentration of aniline present at each time interval. Standard calibration curve of aniline was used which has been described in Sect. 2.4. Aniline concentration was measured between range 200–250 nm wavelength and peak value at 232 nm was taken for analysis. Analysis were done till the concentration of aniline in the solution declined to negligible.

Study of maximum concentration of aniline removal through adsorption onto nZVI in distilled water and in basal salt medium

In an attempt to remove equal concentration of aniline which was found to be removed via biodegradation was tested for maximum removal by adsorption using various concentrations of nZVI. The aniline adsorption experiment was performed similarly as previously performed (refer to 2.3). Keeping the concentration of aniline constant, different concentrations of nZVI ranging from 0.5 to 10 g/L (0.5, 1, 2, 3, 4, 5, 6, 7, 8, 9 and 10 g/L) were added in series of 250 mL volume of Erlenmeyer flasks containing 100 mL of 200 ppm aniline in distilled water and Basal salt medium, respectively. The experiment was conducted in triplet. The adsorption process was carried out for 6 h for each different nZVI concentration. Each solution after 6 h were centrifuged twice at 20,000 rpm for 10 min to remove any nZVI particle and the supernatant were collected in glass vials and were taken for spectral analysis. Amount of aniline adsorbed was calculated as mentioned previously.

Determination of effect of adsorbent dose For constant adsorbate aniline concentration at 200 ppm in both distilled water and basal salt medium, the percentage of removal by various adsorbent concentrations ranging between 0.5 and 10 g/L at the end of 6 h was plotted as bar graph in Originlab 8.0.

Among various concentrations of nZVI ranging between 0.5 and 10 g/L the minimum concentration of nZVI at which maximum removal % of aniline was observed at the end of 6 h was taken for further study. At this time nZVI concentration was kept constant and the concentration of aniline was also kept the same as earlier. The adsorption process was carried out for ten different time intervals viz.15, 30, 45 min, 1, 1.5, 2, 3, 4, 5 and 6 h. UV–Vis spectral analysis of each samples for each time interval were performed similarly as described previously. After determining initial and final concentrations of the solution at each time interval, adsorption percentage was calculated as mentioned previously (refer to Sect. 2.4.).

Effect of contact time, adsorption isotherms and adsorption kinetics were studied similarly as previously mentioned in Sect. 2.4.

Impact of nZVI on acclimatized culture

Toxicity studies were performed using the synthesized nZVI on acclimatized bacterial culture using the method followed by Dey et al. (2015). Cells were cultured overnight in nutrient medium then were centrifuged at 8000 rpm for 10 min and cell pellets obtained were resuspended in basal salt medium solution containing 2 % D-Glucose in 250 mL Erlenmeyer flask at 30 °C incubation temperature and 250 rpm shaking. Cell mass concentration was adjusted to 0.1 at OD_{600}. Culture medium were taken in twelve 20 mL culture tubes containing nZVI concentrations ranging between 0.5 and 10 g/L and another as control having devoid of nZVI. Mouths of the tubes were cotton plugged to prevent contamination and were kept

Sustain. Water Resour. Manag. (2016) 2:143–159

147

under incubation at temperature 30 °C and shaking speed 200 rpm. Cotton plugs allowed free air passage through the system helping in maintaining aerobic condition. After 24 h cell mass concentration of each culture tubes were measured at OD_{600} and were compared with the control.

Combined aniline removal from the system using nZVI together with bacterial inoculums in Basal salt medium

Aniline removal through combined process of adsorption and biodegradation was performed using the same procedure of adsorption by nZVI as previously described, only with the addition of bacterial inoculum in basal salt medium of cell mass concentration value 0.1 measure at OD_{600}. The experiment was performed in 250 mL volume Erlenmeyer flasks for 11 different time intervals viz. 15, 30, 45 min, 1, 1.5, 2, 2.5, 3, 4, 5 and 6 h. Another flask containing equal concentration of aniline subjected to similar conditions but devoid of nZVI and bacterial culture was kept as control to determine loss of aniline if any through evaporation, auto-degradation or photo-degradation. The experiment was conducted in triplet. For all the time intervals initial concentrations of aniline and nZVI were taken the same as previously described and also initial cell mass concentration of all the media was kept at 0.1 measured at OD_{600}.

At the end of each experiment 1 mL of solution was drawn carefully from the top to avoid collection of nZVI. The solution was centrifuged first at 8000 rpm for 5 min to collect only the cell pellet. Cell pellets were re-suspended in distilled water and cell mass concentration was measured at OD_{600}. The supernatant left over was centrifuged again at 20,000 rpm for 10 min to remove any amount of iron nanoparticle present from the solution then the concentration of aniline present in the solution was determined using UV–Vis spectral analysis.

Results and discussion

Characterization of nZVI

Figures 1a, 2b provided represents the FESEM image of CMC-capped nZVI particles. Figure 1a displays sponge-like and porous particle morphology across 5 μm scale, whereas Fig. 2b displays flake like growth viewed through higher resolution at 500 nm scale and looked similar to that which had been previously reported (Yaacob and Kamaruzaman 2012). Figures 1c and 2d represents TEM images of CMC-capped nZVI particles. nZVI particles agglomerated together within CMC to form larger sized particles of 50–100 nm could be observed in Fig. 1c. Figure 1d represents individual particles of sizes ranging

from 3 to 18 nm with maximum particles having size approximately around 10 nm.

Figure 2a shows the image of CMC capped nZVI which is deep black in color and is found to remain stable in normal atmosphere. Figure 2c given below represents the X-ray diffraction (XRD) pattern that confirms phase CMC capped nZVI of according to the JCPDS card number 00-006-0696. Major diffraction peaks was obtained at 44.9̊ and additional peaks at 65.22̊, may be attributed to reflection obtained from Fe(0) lattice planes (110) and bcc Fe(0) (200) (Gangadhar et al. 2012). Based on X-ray diffractogram of Fig. 2c particle size of nZVI was calculated using Scherrer's formula and was found to be approximately 10 nm which was similar to that of obtained through TEM image.

Figure 2e represents FTIR spectroscopy data of CMC capped nZVI particles (black line) and of Sodium carboxymethyl-cellulose powdery mass. Sodium carboxymethyl-cellulose displayed strong and broad O–H stretching around 3200 cm^{-1}, carboxyl group stretching around 1600 cm^{-1} and methyl group stretching around 1450 cm^{-1}. Similar bond stretching were observed around 3200, and 1450 cm^{-1} in nZVI particle sample (black line) but the stretching were of low intensity compared to pure Sodium carboxymethyl-cellulose which indicates proper and uniform capping of nZVI by CMC (Coates 2000).

Abiotic loss of aniline through the system set as control

Approximately 0.25 and 0.6 % of aniline was found to be lost from the system over a period of 3 and 6 h, respectively for all the experiment conducted. The loss could have been in form of photo-degradation, auto-degradation or evaporation from the system. Similar observation have been previously noted by Lyons et al. (1984) (Lyons et al. 1984). Thus approximate standard error of 0.6 % was considered for all experiments performed comprising of nZVI and bacteria over a period of 6 h.

Removal of aniline by adsorption onto nZVI

Effect of contact time

The percentage of aniline removal was found to increase in both the media with increasing contact time. At the end of 3 h 39 % of aniline was found to be removed in medium of distilled water. [refer to Fig. 3a].

Aniline adsorption isotherms

The adsorption of aniline on the nZVI in distilled water solution and basal salt medium were plotted according to
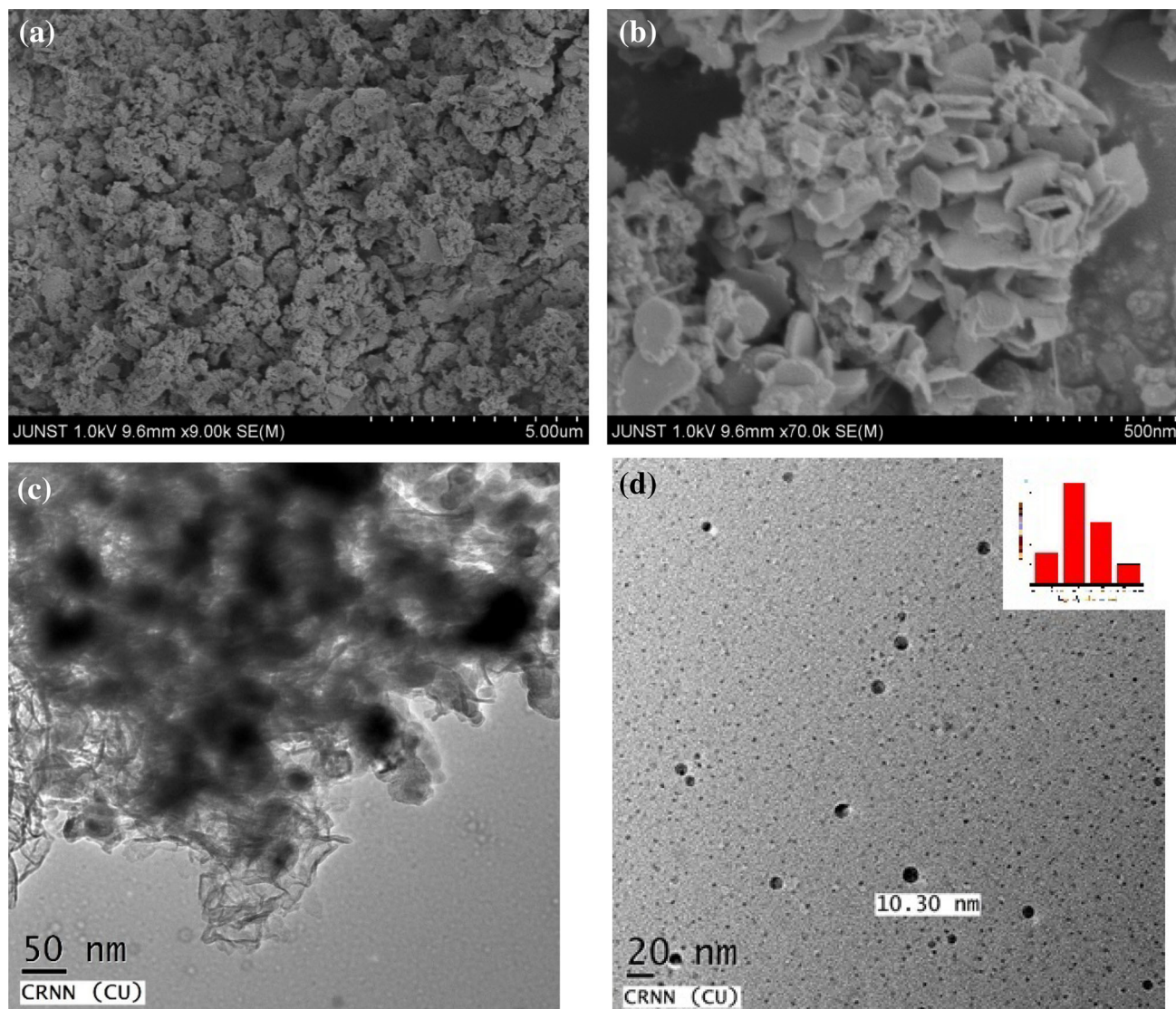
148

Sustain. Water Resour. Manag. (2016) 2:143–159

Fig. 1 **a** FESEM image of nZVI in scale of 5 μm (porous structure); **b** FESEM image of nZVI in scale of 500 nm (flake like structure); **c** TEM image of CMC capped nZVI (individual particle size of 10 nm); **d** TEM image of CMC capped nZVI (particles agglomerated in CMC)

Freundlich, Langmuir and Dubinin-Radushkevich isotherms (Dada et al. 2012; Boparai et al. 2011; Dey et al. 2015). The Langmuir model is usually followed by materials possessing homogenous surface whereas the Freundlich model is normally for a highly heterogeneous surface. (Dada et al. 2012; Dey et al. 2015) Dubinin-Radushkevich isotherm is used to determine nature of adsorption by estimating the energy of adsorption (E_D) (Dada et al. 2012).

The Freundlich isotherm is expressed mathematically as: $q_e = K_f C_e^{1/n}$, where, q_e and C_e represent adsorption capacity at equilibrium concentration (in mg/g) and concentration of adsorbate in solution (mg/L). K_f and n are the empirical constants.

Taking logarithm on both sides we get,

$$\log q_e = \log K_f + \frac{1}{n} \log C_e$$

Langmuir isotherm is represented by the following equation:

$$q_e = \frac{Q_m K_L C_e}{1 + K_L C_e}$$

where Q_m = Maximum adsorption capacity,

K_L = Langmuir constant,

C_e = Concentration of the adsorbate in solution,

q_e = Adsorption capacity at equilibrium solute concentration.
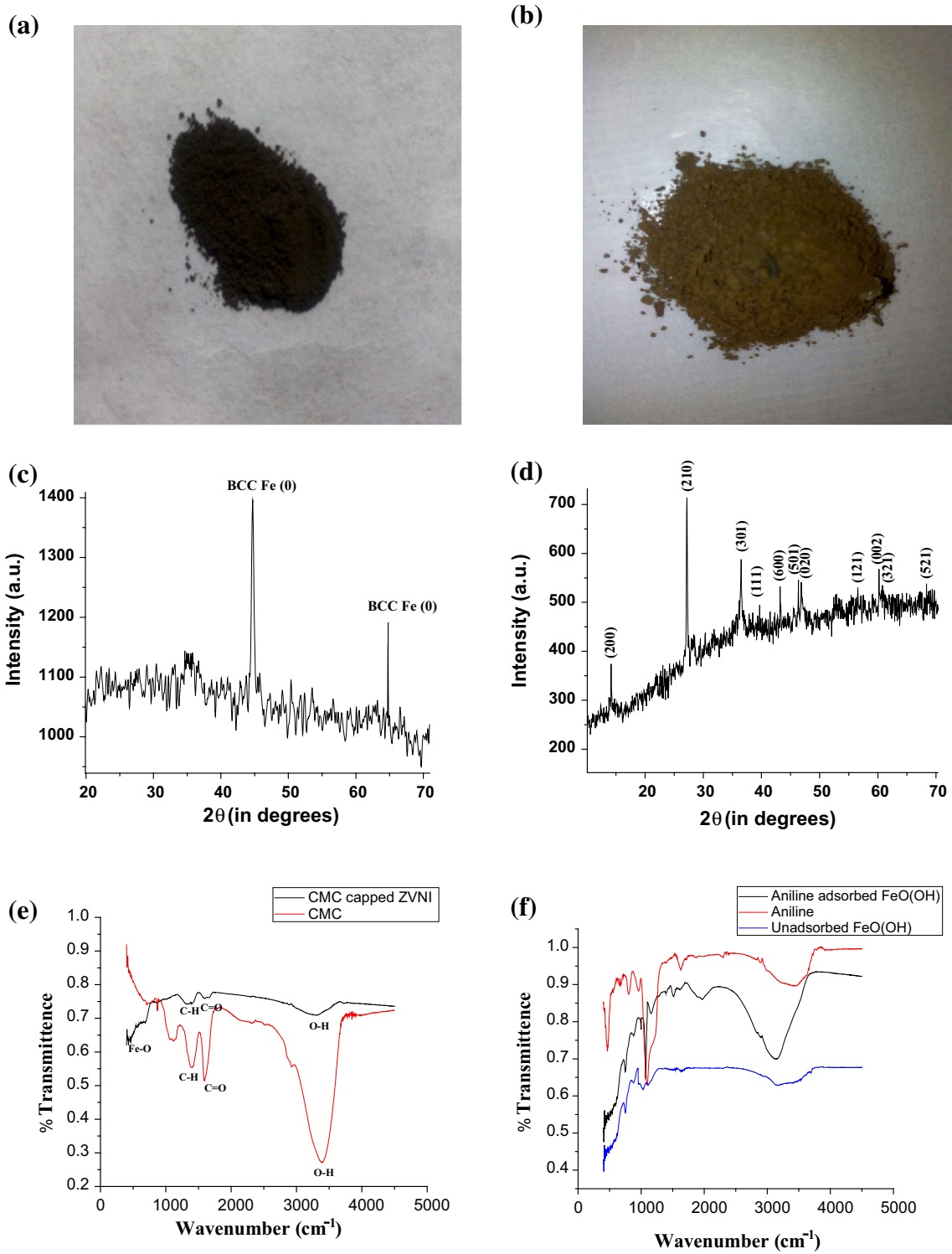
Fig. 2 **a** CMC capped nZVI; **b** nZVI after adsorption experiment (FeO(OH)); **c** X-RD of CMC capped nZVI; **d** X-RD of nZVI after aniline adsorption; **e** FTIR spectra of CMC capped nZVI; **f** FTIR spectra of aniline adsorbed to nZVI surface after adsorption
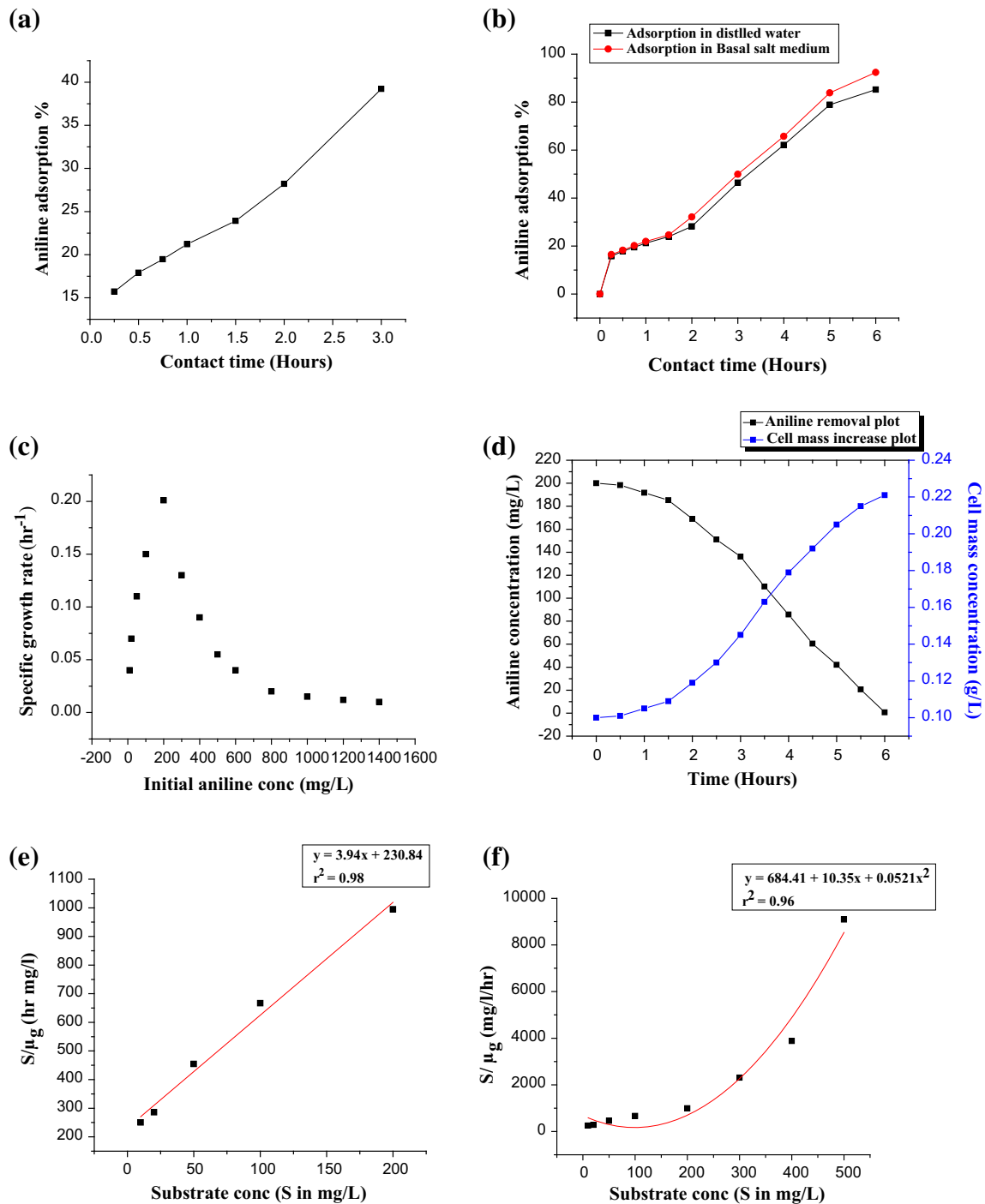
(a)

(b)

(c)

(d)

(e)

(f)

Fig. 3 a Effect of aniline removal through adsorption to 1 g/L nZVI in different time intervals; **b** Effect of aniline removal through adsorption to 5 g/L nZVI in different time intervals; **c** Effect of initial aniline concentration on specific growth rate of *P. putida* MTCC 1194; **d** growth of cell mass and subsequent aniline removal; **e** monod kinetics plot for *P. putida* MTCC 1194 in presence of substrate aniline; **f** Haldane kinetics plot for *P. putida* in presence of substrate aniline

The above equation can be further written as:

$$\frac{C_e}{q_e} = \frac{1}{Q_m K_L} + \frac{C_e}{Q_m}$$

or, $\frac{1}{q_e} = \frac{1}{C_e Q_m K_L} + \frac{1}{Q_m}$

On plotting $1/q_e$ vs. $1/C_e$, from the above equation, which is in the form of the equation of straight line, the values of K_L and Q_m were determined.

Dubinin-Radushkevich isotherm is represented by the the following equation:

Table 1 Adsorption isotherm results for aniline adsorption to nZVI

Isotherm models	Freundlich			Langmuir			Dubinin-Radushkevich		
Medium of adsorption	K_f (Freundlich constant)	n (degree of heterogeneity)	r^2	Q_m (mg/g)	K_L (L/mg)	r^2	q_D	E_D (J)	r^2
Distilled water (1 g/L nZVI)	0.377	0.44	0.94	17.42	1.29	0.94	22.88	49.09	0.96
Distilled water (5 g/L nZVI)	7.04	1.04	0.86	43.10	0.99	0.98	45.74	49.09	0.99
Basal salt medium (5 g/L nZVI)	7.99	1.38	0.79	43.85	0.97	0.97	46.15	48.98	0.99
Basal salt medium (with *P. putida* and nZVI)	2.45	0.19	0.98	25.01	1.91	0.99	23.49	53.38	0.99

Table 2 Kinetics parameter for aniline removal through adsorption on nZVI

Medium of adsorption	Rate constant (k_1)	r^2	Rate constant (k_2)	r^2
Distilled water (with 1 g/L nZVI)	0.73	0.99	0.12	0.85
Distilled water (with 5 g/L nZVI)	0.72	0.97	0.0035	0.49
Basal salt medium (with 5 g/L nZVI)	0.74	0.97	0.0029	0.49
Basal salt medium with bacteria (with 1 g/L nZVI)	0.47	0.48	0.40	0.99

$$qe = qD \exp(-B_D[RT \ln(1 + 1/Ce)])$$

where, B_D is related to the free energy of sorption per mole of the sorbate.

q_D = Dubinin-Radushkevich isotherm constant related to the degree of adsorbate adsorption by the adsorbent surface.

The linear form of equation is written as:

$$\ln q_e = \ln q_D - 2B_DRT \ln (1 + 1/C_e)$$

Using the above equation a plot of ln q_e vs $2B_D$ RT ln $(1 + 1/C_e)$ is made which generates a straight line. Using the value of $2B_D$, apparent energy of adsorption E_D was calculated from the relation $E_D = \sqrt{1/2B_D}$

The results are listed in Table 1. From the results isotherm plot of aniline adsorption to nZVI surface was found to fit most perfectly to Langmuir model compared to Freundlich based on r^2 value, thus predicting homogenous surface of nZVI. The value Q_m obtained for nZVI in distilled water solution was 17.42 mg/g. With the help of Dubinin-Radushkevich isotherm model plot E_D value of the entire adsorption experiment was found to be within range less than 8 kJ thus predicting the nature of adsorption to be physical adsorption.

Aniline adsorption kinetics in distilled water solution

To determine the rate of aniline removal due to adsorption to nZVI in distilled water as well as in basal media solution three kinetic models were studied viz. pseudo first order, pseudo second order (Ho and McKay 1998; Dey et al. 2015).

The Table 2 represents the rate constant k and r^2 value for the respective kinetic models plotted for aniline removal through adsorption in distilled water and basal media solution, respectively. The r^2 value depicts the degree of correlation of a kinetic model. The higher is the r^2 value higher is the accurateness of following the kinetics model.

Thus on performing the kinetic studies and fitting the results accordingly to the three foresaid kinetic models, it was found that the r^2 value was highest for pseudo first order kinetic model in comparison to pseudo second order for adsorption. Thus, it was concluded that the rate of aniline removal through adsorption to nZVI followed the pseudo first order kinetic model.

Post adsorption characterization of adsorbent

nZVI after adsorption experiment was found to form deep brown mass with slightly agglomerated texture as shown in Fig. 2b. Figure 2d shows the X-ray diffraction (XRD) pattern that predicts and confirms the formation of FeO(OH) according to the JCPDS card number 00-044-1415.

Major diffraction peak was obtained at 27°(210) and additional peaks at 14.1°(200), 36.29°(301), 38.06°(111), 43.34°(600), 46.77°(501), 46.91°(020), 56.63°(121), 60.26°(020), 60.68°(321), 68.36°(521), may be attributed to reflection obtained from the provided lattice planes in brackets.

Figure 2f represents comparison of FTIR spectra of Aniline (red line), aniline adsorbed FeO(OH) (in black) and unadsorbed FeO(OH) (in blue). For aniline (represented in red) N–H stretching were observed around 3400–3250 cm^{-1}, small N–H bend was seen at 1650–1580 cm^{-1} and overlapping C–N stretch and N–H

152

Sustain. Water Resour. Manag. (2016) 2:143–159

wag is observed around 900–1300 cm^{-1}. For aniline adsorbed to FeO(OH) (represented in black), wide overlapping O–H and N–H stretching was observed around 2700–3400 cm^{-1}, small N–H bend was seen at 1650–1580 cm^{-1} similar to previous bare aniline and distinct C–N stretch and N–H wag was observed around 1250 and 1000 cm^{-1}, thus confirming adsorption on aniline onto FeO(OH) surface. Whereas unadsorbed FeO(OH) is found to have only O–H stretching around 3000 cm^{-1}. (Coates 2000)

Mechanism of aniline adsorption to nZVI surface

Aniline at neutral pH possesses a resonating structure. Lone pair of electron present on nitrogen is contributed towards the benzene ring which results in forming partial double bond of N=O and partial δ^+ is generated on nitrogen atom whereas the lone pair of electron contributed by nitrogen moves continuously through ortho and para positions of aniline (refer to Fig. 5).

CMC is reported to stabilizes the nanoparticles through the accelerating nucleation of Fe atoms during the formation of nZVI particles and, subsequently, forming a bulky and negatively charged layer via sorption of CMC molecules onto the nZVI particles, thereby preventing the nanoparticles from agglomeration through electrosteric stabilization (He and Zhao 2007) (refer to Fig. 4a, b). And also size of nZVI is reported to decrease with increase in CMC/Fe ion ratio (He and Zhao 2007). On adding to water the entire CMC capped over nZVI surface dissolves and naked nZVI surface is exposed aerobic water thus undergoes oxidation and forms outer shell of FeO(OH) as confirmed through X-RD analysis (refer to Fig. 4c). As previously mentioned freshly oxidized nZVI have been reported to possess high adsorbing potential (Eagleson 1994).

The specialty of nZVI aiding adsorption lies in the fact that in the nano regime, the number of unsatisfied bonds (i.e. number of unsatisfied electron pairs) increases. Moreover, with decrease in size, the surface to volume ratio increases drastically. Theoretically, it can be considered that the nZVI nanoparticles have negative charged surface. Thus, the surface charge of nZVI aids to electrostatic attraction of positively charged Ph–NH_2^+. The enhanced adsorption may be attributed to the combined effect of dangling bonds, high surface-to-volume ratio and electrostatic attractive force as the physical properties affecting the adsorption. Apart from these, the biological factors and micro organisms are observed to enhance the adsorption even more. These are discussed in details in the subsequent sections.

Iron contains plenty of vacant d-orbitals, thus has the ability to bond with electron clouds using coordinate bond

formation. Oxygen bound to iron as Fe=O contains two lone pair of electrons which confers charge to oxygen as δ^-. Similarly hydroxide group bound to iron as Fe–OH also possesses two lone pairs of electron of oxygen. Thus in spite of having vacant d-orbital of iron, the nature of FeO(OH) surface becomes negatively charged because of having plenty of lone pair of electrons. Thus during adsorption process δ^+ charge possessing nitrogen atom of aniline binds onto the electron cloud generated through plenty of lone pair of electron present on FeO(OH) surface through temporary coordinate bond (refer to Fig. 5).

Acclimatization of *Pseudomonas putida* to aniline and study of growth kinetics

In normal environment bacterial cells do not easily metabolize toxic substances, they can be made to metabolize only after getting through a proper phase of acclimatization which is time and concentration dependent. Initially the cells are required to be grown in nutrient broth to generate a good amount of cell mass. Later they are transferred into basal medium solution containing trace elements which are necessary to sustain growth and induce essential enzymes. The basal medium is supplemented with 2 % D-Glucose and small concentration (10 ppm) of toxic substance (aniline) to which cells are required to be acclimatized. At first the cells metabolizes D-Glucose since it is the simplest form of carbon source and cell mass is increased. Once all the D-Glucose is consumed cell mass concentration reaches saturation for a while. Then later slowly, starting from a few number of colonies, cells acquire the ability to metabolize toxic substrate aniline through inducing activity of essential enzymes like Cytochrome P_{450} cam (CYP101) which help metabolize toxic substrates (Keller et al. 1972). Thus in absence of simple carbon source D-Glucose at this stage, the cells which are able to use toxic substrate aniline as their sole carbon source, undergo proper growth and division.

Cells were serially acclimatized to higher aniline concentration for every 10 days till 2 month with each time concentration of aniline doubled with respect to initial. After 2 month of acclimatization phase growth rate μ_g was determined for the cells in different aniline concentrations 10, 50, 100, 200, 300, 400 and 500 ppm. The Fig. 3c represents the growth rate of cells with respect to aniline concentration. Maximum observable growth rate was found at aniline concentration 200 ppm. From 300 ppm cell growth rate started to decline as evident from the above figure. This phenomena proved the substrate inhibitory nature of aniline to the culture similar to previously reported for phenol and catechol (Kumar et al. 2005; Bakhshi et al. 2011).

Yield coefficient is the amount of increase in cell mass with respect to amount of substrate consumed (Kumar et al.
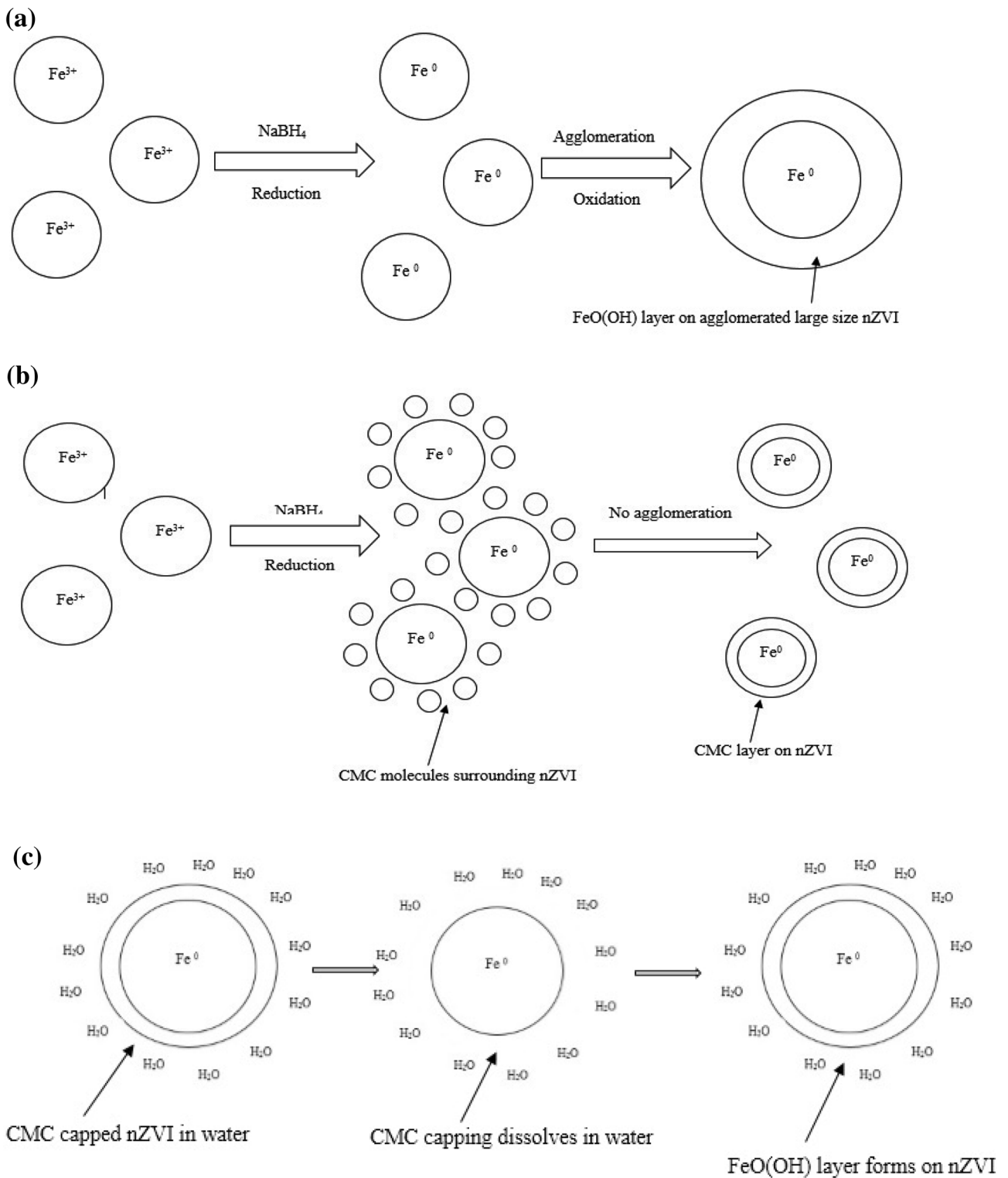
Fig. 4 a Mechanism of formation of CMC capped nZVI and its behavior after synthesis; **b** mechanism of formation of uncapped nZVI and its behavior after synthesis; **c** mechanism of dissolution of CMC from the surface of nZVI in water and formation of shell like layer of FeO(OH) on nZVI
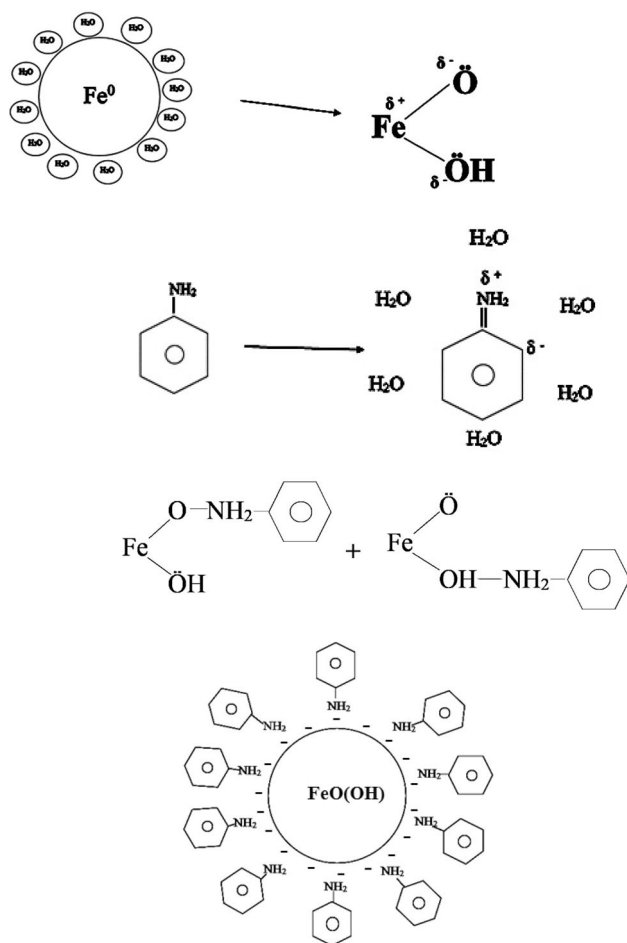
Fig. 5 Mechanism of aniline adsorption onto nZVI surface

2005; Bakhshi et al. 2011). Yield coefficient ($Y_{x/s}$) was determined to be 0.613 mg/mg by plotting cell concentration vs substrate utilization. Two growth kinetic models viz. Monod and Haldane were exploited to determine the cell growth parameters. Monod kinetic model is simple growth model used for non-inhibitory substrates which is represented as (Kumar et al. 2005; Bakhshi et al. 2011):

$$\mu_g = \frac{\mu_{max}S}{K_S + S}$$

where, μ_g = Specific growth rate, μ_{max} = Maximum specific cell growth rate,

K_s = Hall saturation constant, S = Non inhibitory substrate concentration.

The above equation can be linearized as:

$$\frac{S}{\mu_g} = \frac{K_S}{\mu_{max}} + \frac{S}{\mu_{max}}$$

By plotting (S/μ_g) vs S value of μ_{max} and K_s were determined. (refer to Fig. 3e)

Haldane kinetics model is generally used for growth inhibitory substrates which is represented as (Kumar et al. 2005; Bakhshi et al. 2011):

$$\mu_g = \frac{\mu_{max}S}{K_S + S + \frac{S^2}{K_i}}$$

where, K_i = inhibition coefficient, and all other parameters are same as mentioned in Monod kinetics model.

The above equation can be linearized to form a parabolic equation:

$$\frac{S}{\mu_g} = \frac{K_S}{\mu_{max}} + \frac{S}{\mu_{max}} + \frac{S^2}{\mu_{max}K_i}$$

By plotting (S/μ_g) vs S in polynomial parabolic function fitting model, values of μ_{max} and K_s and K_i were determined. (refer to Fig. 3f)

The Table 3 represents the growth parameter values obtained by plotting Monod and Haldane kinetics model.

Since maximum observable growth rate was obtained at 200 ppm aniline concentration (refer to Fig. 3c), the same concentration was used for further studies. Around 99 % of 200 ppm aniline was found to be removed within 6 h. (Refer to Fig. 3d) The rate of aniline biodegradation was plotted in first order kinetics and the rate was found to be 0.51 h^{-1}. The acclimatized cells were found to have shorter lag phase and sustained exponential phase till 4 h after which the cells were seen to slowly entering into stationary phase. (Refer to Fig. 3d)

Sorption study of aniline onto cell biomass

Approximately 67 % of aniline was estimated to be converted into cell biomass by comparing the total carbon content of aniline removed and *P. putida* cell biomass growth (Bratbak and Dundas 1984) incurred within time period of 6 h and the rest 33 % were estimated to have been collectively undergone sorption onto biomass, metabolized into energy by the actively growing cell mass.

Removal of maximum aniline through adsorption

Effect of adsorbent dose

On increasing adsorbent concentration percentage of aniline removal also increased and the maximum percentage of aniline removal was achieved at 5 g/L nZVI concentration (85 % in distilled water and 92 % in basal salt media) and after which the removal percentage remained almost constant for the rest of the higher nZVI concentrations. (refer to Fig. 6a)

Table 3 Monod and Haldane model parameters

Monod model			Haldane model			
μ_{max} (h^{-1})	K_s (mg/L)	r^2	μ_{max} (h^{-1})	K_s (mg/L)	K_i (mg/L)	r^2
0.25	58.57	0.98	0.11	67.56	184.30	0.96

Effect of contact time

The percentage of aniline removal was found to increase in both the media with increasing contact time. At the end of 6 h 85 % of aniline was found to be removed in medium of distilled water and 92 % was removed in basal salt medium. (refer to Fig. 3b).

Aniline adsorption isotherms

The adsorption of aniline on the nZVI in distilled water solution and basal salt medium were plotted according to Freundlich, Langmuir and Dubinin-Radushkevich isotherms. The results are listed in Table 1. From the results isotherm plot of aniline adsorption to nZVI surface was found to fit most perfectly to Langmuir model (refer to additional information Fig. 4b) compared to Freundlich (refer to additional information Fig. 4a) based on r^2 value, thus predicting homogenous surface of nZVI. The value Q_m obtained for nZVI in distilled water solution was 43.10 mg/g (refer to Table 1) and in basal salt media was found to be 43.85 mg/g (refer to Table 1). With the help of Dubinin-Radushkevich isotherm model plot (refer to additional information Fig. 4c) E_D value of the entire adsorption experiment was found to be within range less than 8 kJ (refer to Table 1) thus predicting the nature of adsorption again as previously determined to be physical adsorption.

Kinetics study of aniline removal through adsorption

To determine the rate of aniline removal due to adsorption to nZVI in distilled water as well as in basal media solution three kinetic models were studied viz. pseudo first order and pseudo second order.

The results are listed in Table 2. The r^2 value depicts the degree of correlation of a kinetic model. The higher is the r^2 value higher is the accurateness of following the kinetics model.

Thus on performing the kinetic studies and fitting the results accordingly to the two foresaid kinetic models, it was found that the r^2 value was highest for pseudo first order kinetic model in comparison to pseudo second order for adsorption in both distilled water and in basal media solution. Thus, it was concluded that the rate of aniline removal through adsorption to nZVI followed the pseudo first order kinetic model.

From the figure and table it was also observed that that rate of aniline removal in basal media solution was slightly higher than that of distilled water. This can be attributed due to the presence of various ions in the solution which cumulatively helped to increase the adsorptive capacity of nZVI.

Impact of nZVI on acclimatized culture

After 24 h of incubation with different concentration of nZVI, cell mass concentration was found to be higher in all the culture tubes incubated with nZVI compared to the control which was devoid of nZVI. The cell mass concentration was found to increase with increase in the concentration of nZVI, however it became constant with increasing concentration of nZVI after reaching the concentration of 4 g/L of nZVI. (refer to Fig. 6b)

Thus we can say that nZVI was not only found to be completely non-toxic to the cells but also acted as a growth inducer. Under aerobic condition nZVI rapidly reacted with oxygen and water generating an outer shell of FeO(OH) around the surface of nZVI (Zhang 2003). FeO(OH) has also previously been reported to be non-toxic and also growth promoter to *Pseudomonas aeruginosa* (Borcherding et al. 2014; Kostka et al. 2002; Dehner et al. 2010) and also might have acted as electron acceptor to the cells as similar property was previously described by Obuekwe and Westlake (1982) on *Pseudomonas* sp. (Obuekwe and Westlake 1982).

Bacterial culture together with nZVI for aniline removal in Basal salt media solution

At the end of 2.5 h around 99 % aniline was found to be removed from the system consisting of both nZVI and *P. putida* cells. Figure 6d shows the comparison of percentage of aniline removal among the four different systems studied in the present work. The figure clearly indicates the maximum rate of aniline removal is obtained from the system composed of both nZVI and *P. putida* cells. The Fig. 6a represents the increase in cell mass concentration value across 2.5 h period and subsequent aniline removal from combined system composed of aniline and nZVI. Figure 6b draws the comparison of the rate of increase of cell mass in the two distinct systems. From the figure it is evident that cells in presence of nZVI in their surrounding had substantially higher growth rate
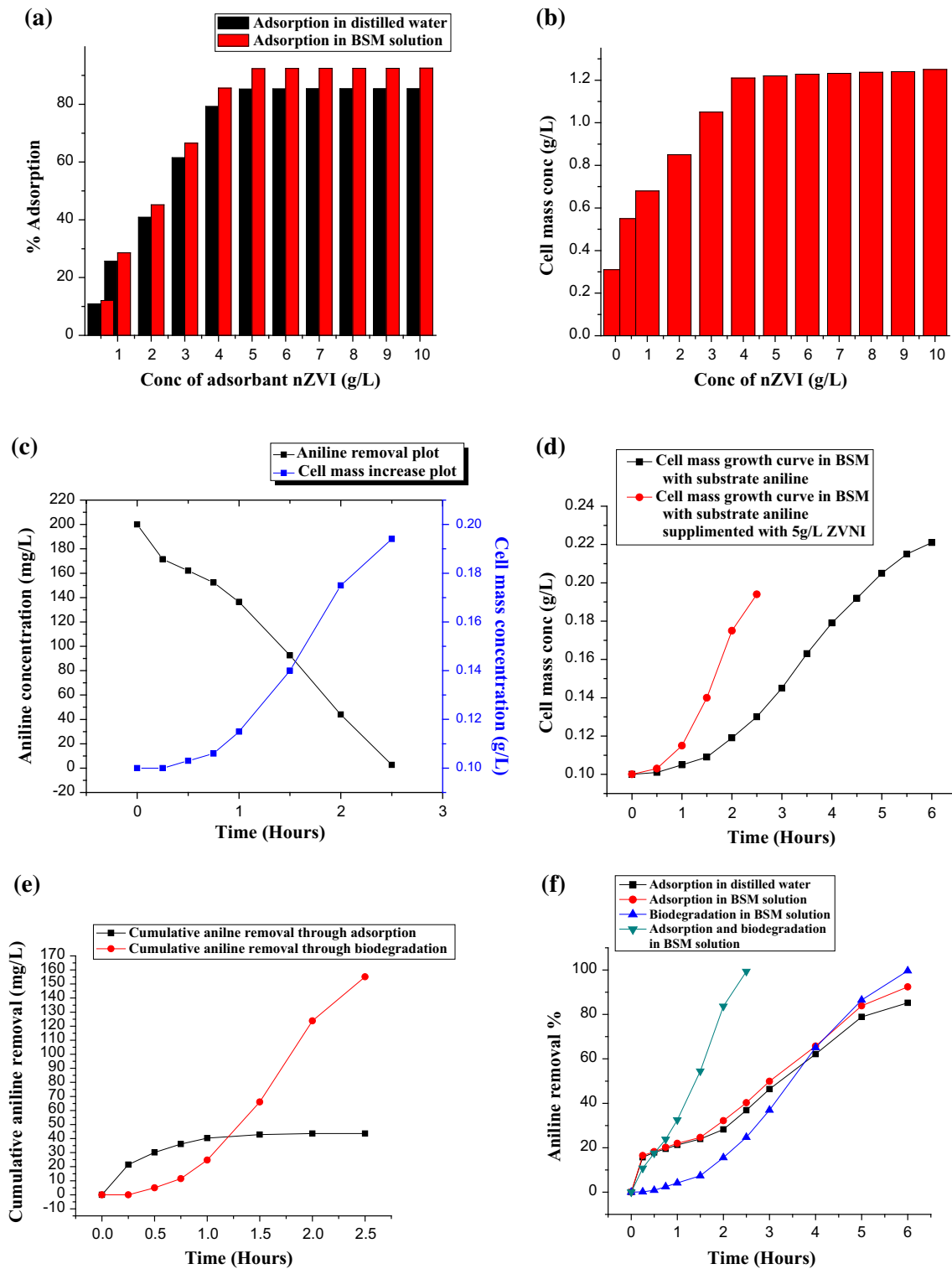
Fig. 6 a Cell mass growth and subsequent aniline removal in system containing nZVI; b comparison of cell growth alone with cell growth containing nZVI; c estimated amount of aniline removal through

separate sorption and biodegradation; d comparison of aniline removal % in different media

compared to cells present alone and owing to higher cell growth rate aniline removal rate was also significantly higher.

During the first 30 min growth in cell mass was found to be negligible and aniline removal was assumed to be entirely through adsorption onto nZVI surface (refer to

Table 4 Comparison of First order growth rate constant for cells and first order rate constant for aniline removal

Medium of cell growth	1st order cell growth rate (h^{-1})	1st order cell growth r^2 value	1st order aniline removal rate (h^{-1})	1st order aniline removal r^2 value
Basal salt medium	0.21	0.99	0.51	0.97
Basal salt medium (with 5 g/L nZVI)	0.40	0.99	0.76	0.98

Fig. 6c). At the end of 2 h approximately 61 % of aniline was estimated to be converted into cell biomass by comparing the total carbon content of aniline removed and *P. putida* cell biomass present in the system (Bratbak and Dundas 1984) while the rest 39 % were estimated to have been collectively undergone adsorption onto nZVI surface, sorption onto cell biomass and metabolized into energy by the actively growing cell mass.

Similarly for various time intervals by comparing the total carbon content of aniline removed and *P. putida* cell biomass present in the system approximate amount of aniline removed by biodegradation and collective sorption onto nZVI particles and biomass were segregated. The amount of aniline lost in metabolism of growing cells mass were assumed negligible this time to avoid complication in calculation.

Using the respective segregated values graph was plotted together for cumulative percentage of removal of aniline through biodegradation and through sorption in the same system (refer to Fig. 6c). The figure show that during the lag phase of growth of the cells aniline removal through sorption was maximum, preferably because of adsorption onto nZVI surface. And as soon as rapid growth rate reached for the cells the rate of adsorption declined and reached equilibrium very soon. Two factors might have been responsible together for the decline in the rate of aniline adsorption viz. firstly increase in the cell mass concentration reduced the surface area of contact of aniline onto nZVI particles and secondly the time taken by the cells for intake of aniline might have been lower than the time taken for adsorbing onto the surface of nZVI. The adsorption onto nZVI particles, bio-sorption and biodegradation might have simultaneously taken place together in the system once the system gained equilibrium. But it is not clear whether nZVI present along-with bacteria facilitated transport of aniline into the cells.

The calculated values for aniline removed by the cells were plotted in first order kinetics model and the value of "k" was found to be and which on comparison to the previous 1.5 times higher than the normal rate of bacterial aniline removal. Comparison on cell growth rate and aniline removal rate are listed in Table 4.

Collective sorption values for aniline removal in presence of aniline consuming bacteria and nZVI were also plotted according to the previously mentioned isotherms and kinetic models. The results linearly fitted to all the model isotherms. The values of collective sorption isotherms are represented in Table 1. From Langmuir isotherm plot Q_m value was obtained to be 25 mg/g which is substantially lower than adsorption process without presence of bacteria. The value E_D obtained from Dubinin-Radushkevich for collective sorption was comparable to the previously predicted E_D value confirming the nature of sorption to be only physical.

The Table 2 represents the rate constant k and r^2 value of the respective kinetic models for collective aniline sorption. The values fitted more linearly to pseudo-second order kinetics model than pseudo-first order model as evident from the value of r^2, thus indicating presence of cell mass had a clear impact on the system of adsorption of aniline to nZVI surface which leaves scope for further studies.

Conclusion

The present work was intended to study the nature of aniline removal from water using a combined system of nZVI and *P. putida*. nZVI was found to possess very good adsorptive property due to its high surface to volume ratio which is quintessential for aniline removal and it also proved to be growth inducer for *P. putida* strain. On using combined system containing nZVI and *P. putida*, the removal of aniline was found to be substantially higher than individual systems containing only nZVI or *P. putida* strain. Thus the present study leaves bright prospect for further studies on enhancing removal of toxic pollutants from wastewater together in a system comprising of nZVI and micro-organisms on proper optimization.

References

Adami S, Fakhri A (2013) Adsorption of 4-chloro-2-nitrophenol by zero valent ironnanoparticles and Pd-doped zero valent iron nanoparticles surfaces: isotherm, kinetic and mechanism modeling. J Phys Chem Biophys 3(115):0398–2161

158

Sustain. Water Resour. Manag. (2016) 2:143–159

Al-Johani H, Salam MA (2011) Kinetics and thermodynamic study of aniline adsorption by multi-walled carbon nanotubes from aqueous solution. J Colloid Interface Sci 360(2):760–767

Ang EL, Obbard JP, Zhao H (2009) Directed evolution of aniline dioxygenase for enhanced bioremediation of aromatic amines. Appl Microbiol Biotechnol 81(6):1063–1070

Anotai J, Lu MC, Chewpreecha P (2006) Kinetics of aniline degradation by Fenton and electro-Fenton processes. Water Res 40(9):1841–1847

Bakhshi Z, Najafpour G, Kariminezhad E, Pishgar R, Mousavi N, Taghizade T (2011) Growth kinetic models for phenol biodegradation in a batch culture of Pseudomonas putida. Environ Technol 32(16):1835–1841

Beard RR, Noe JT (1981) Aromatic Nitro and Amino Compounds. In: Patty's industrial hygiene and toxicology, vol 2. Wiley, New York, pp 2413–2489

Boparai HK, Joseph M, O'Carroll DM (2011) Kinetics and thermodynamics of cadmium ion removal by adsorption onto nano zerovalent iron particles. J Hazard Mater 186(1):458–465

Borcherding J, Baltrusaitis J, Chen H, Stebounova L, Wu CM, Rubasinghege G, Comellas AP (2014) Iron oxide nanoparticles induce Pseudomonas aeruginosa growth, induce biofilm formation, and inhibit antimicrobial peptide function. Environ Sci Nano 1(2):123–132

Bratbak G, Dundas I (1984) Bacterial dry matter content and biomass estimations. Appl Environ Microbiol 48(4):755–757

Buddhika G, Naresh S, Peter S (2011) Degradation of chlorinated phenols by zero valent iron and bimetals of iron: a review. Environ Eng Res 16(4):187–203

Coates J (2000) Interpretation of infrared spectra, a practical approach. Encycl Anal Chem, pp 10815–10837. doi:10.1002/9780470027318.a5606

Dada AO, Olalekan AP, Olatunya AM, Dada O (2012) Langmuir, freundlich, temkin and dubinin–radushkevich isotherms studies of equilibrium sorption of Zn2 + unto phosphoric acid modified rice husk. J Appl Chem 3(1):38–45

Dehner CA, Awaya JD, Maurice PA, DuBois JL (2010) Roles of siderophores, oxalate, and ascorbate in mobilization of iron from hematite by the aerobic bacterium Pseudomonas mendocina. Appl Environ Microbiol 76(7):2041–2048

Deschenes LA, David A (2000) Vanden Bout University of Texas, Austin. Origin 6.0: Scientific Data Analysis and Graphing Software Origin Lab Corporation (formerly Microcal Software, Inc.). Web site: www originlab com. Commercial price: 595. Academicprice: 446. J Am Chem Soc 122(39):9567–9568

Dey S, Bhattacharjee S, Bose RS, Ghosh CK (2015) Room temperature synthesis of hydrated nickel (III) oxide and study of its effect on Cr(VI) ions removal and bacterial culture. Appl Phys A 119(4):1343–1354

Donald L Wise. In situ bioremediation of xenobiotics. Page 141. Bioremediation of contaminated soil. ISBN 0-8247-0333-2. Edition 2000

Eagleson M (1994) Concise encyclopedia chemistry. Walter de Gruyter, Berlin, New York (translated from German)

Elliott DW, Zhang WX (2001) Field assessment of nanoscale bimetallic particles for groundwater treatment. Environ Sci Technol 35(24):4922–4926

Gangadhar B, Basu H, Manisha V, GRK N, AVR R (2012) Remediation of malathion contaminated soil using zero valent iron nano-particles. Am J Anal Chem 3(1):76–82

Fiore JV, Babineau RA (1977) Effect of an activated carbon filter on the microbial quality of water. Appl Environ Microbiol 34(5):541–546

Fuchs K, Schreiner A, Lingens F (1991) Degradation of 2-methylaniline and chlorinated isomers of 2-methylanili by Rhodococcusrhodochrous strain CTM. J Gen Microbiol 137(8):2033–2039

Greenlee LF, Torrey JD, Amaro RL, Shaw JM (2012) Kinetics of zero valent iron nanoparticle oxidation in oxygenated water. Environ Sci Technol 46(23):12913–12920

Hallas LE, Alexander M (1983) Microbial transformation of nitroaromatic compounds in sewage effluent. Appl Environ Microbiol 45(4):1234–1241

He K (2012) A calculation of the environmental footprint of a granular activated carbon regeneration facility. In: Climate and Energy section. Environmental Sciences Senior Thesis Symposium. UC Berkeley Environmental Sciences, 22 April 2012

He F, Zhao D (2007) Manipulating the size and dispersibility of zerovalent iron nanoparticles by use of carboxymethyl cellulose stabilizers. Environ Sci Technol 41(17):6216–6221

Ho YS, McKay G (1998) Kinetic models for the sorption of dye from aqueous solution by wood. Process Saf Environ Prot 76(2):183–191

Honghai WU, Yiying LIN, Jiayi WU, Lixuan ZENG, Dingcai ZENG, Juan DU (2008) Surface adsorption of iron oxide minerals for phenol and dissolved organic matter. Earth Sci Front 15(6):133–141

Howard PH (1989) Handbook of environmental fate and exposure data for organic chemicals, Vol. I. Large production and priority pollutants. Lewis Publishers Inc, Chelsea, pp 44–52

Jang MH, Lim M, Hwang YS (2014) Potential environmental implications of nanoscale zero-valent iron particles for environmental remediation. Environ Health Toxicol 29:e2014022

Keller RM, Wüthrich K, Debrunner PG (1972) Proton magnetic resonance reveals high-spin iron (II) in ferrous cytochrome P450cam from Pseudomonas putida. Proc Natl Acad Sci 69(8):2073–2075

Kim J, Li W, Philips BL, Grey CP (2011) Phosphate adsorption on the iron oxyhydroxides goethite (α-FeOOH), akaganeite (β-FeOOH), and lepidocrocite (γ-FeOOH): a 31 P NMR Study. Energy Environ Sci 4(10):4298–4305

Kinouchi TAKEMI, Ohnishi YOSHINARI (1983) Purification and characterization of 1-nitropyrene nitroreductases from Bacteroidesfragilis. Appl Environ Microbiol 46(3):596–604

Kostka JE, Dalton DD, Skelton H, Dollhopf S, Stucki JW (2002) Growth of iron (III)-reducing bacteria on clay minerals as the sole electron acceptor and comparison of growth yields on a variety of oxidized iron forms. Appl Environ Microbiol 68(12):6256–6262

Kumar A, Kumar S, Kumar S (2005) Biodegradation kinetics of phenol and catechol using Pseudomonas putida MTCC 1194. Biochem Eng J 22(2):151–159

Li S, Li T, Xiu Z, Jin Z (2010) Reduction and immobilization of chromium (VI) by nano-scale Fe0 particles supported on reproducible PAA/PVDF membrane. J Environ Monit 12(5):1153–1158

Liang W, Dai C, Zhou X, Zhang Y (2014) Application of zero-valent iron nanoparticles for the removal of aqueous zinc ions under various experimental conditions. PLoS One 9(1):e85686

Lin KS, Chang NB, Chuang TD (2008) Fine structure characterization of zero-valent iron nanoparticles for decontamination of nitrites and nitrates in wastewater and groundwater. Sci Technol Adv Mater 9(2):025015

Loidl M, Hinteregger C, Ditzelmüller G, Ferschl A, Streichsbier F (1990) Degradation of aniline and monochlorinated anilines by soil-born Pseudomonas acidovorans strains. Arch Microbiol 155(1):56–61

Lyons CD, Katz S, Bartha R (1984) Mechanisms and pathways of aniline elimination from aquatic environments. Appl Environ Microbiol 48(3):491–496

Madhavi V, Prasad TNVKV, Reddy AVB, Reddy BR, Madhavi G (2013) Application of phytogenic zerovalent iron nanoparticles

in the adsorption of hexavalent chromium. Spectrochim Acta Part A Mol Biomol Spectrosc 116:17–25

Martin JE, Herzing AA, Yan W, Li XQ, Koel BE, Kiely CJ, Zhang WX (2008) Determination of the oxide layer thickness in core-shell zerovalent iron nanoparticles. Langmuir 24(8):4329–4334

Mueller NC, Braun J, Bruns J, Černík M, Rissing P, Rickerby D, Nowack B (2012) Application of nanoscale zero valent iron (NZVI) for groundwater remediation in Europe. Environ Sci Pollut Res 19(2):550–558

Najafpour G (2015) 10.5. Optical cell density, page 332. Biochemical Engineering and Biotechnology. 2nd edn ISBN: 978-0-444-63357-6

Nassar NN, Ringsred A (2012) Rapid adsorption of methylene blue from aqueous solutions by goethite nanoadsorbents. Environ Eng Sci 29(8):790–797

Obuekwe CO, Westlake DWS (1982) Effects of medium composition on cell pigmentation, cytochrome content, and ferric iron reduction in a *Pseudomonas* sp. isolated from crude oil. Can J Microbiol 28(8):989–992

Otte K, Schmahl WW, Pentcheva R (2013) DFT + U study of arsenate adsorption on FeOOH surfaces: evidence for competing binding mechanisms. J Phys Chem C 117(30):15571–15582

Patil SS, Shinde VM (1988) Biodegradation studies of aniline and nitrobenzene in aniline plant wastewater by gas chromatography. Environ Sci Technol 22(10):1160–1165

Prabu D, Parthiban R, Senthil Kumar P, Kumari N, Saikia P (2016) Adsorption of copper ions onto nano-scale zero-valent iron impregnated cashew nut shell. Desalination Water Treat 57(14):6487–6502

Qiu X, Fang Z, Yan X, Cheng W, Lin K (2013) Chemical stability and toxicity of nanoscale zero-valent iron in the remediation of chromium-contaminated watershed. Chem Eng J 220:61–66

Rabert WS 1991 Memorandum from William Rabert, Environmental Effects Branch, to John Harris, Chemical Testing Branch. Subject: Review of Daphnia magna 21-Day Life Cycle Toxicity Test on Aniline. Jan 8, 1991

Shimizu A, Tokumura M, Nakajima K, Kawase Y (2012) Phenol removal using zero-valent iron powder in the presence of dissolved oxygen: roles of decomposition by the Fenton reaction and adsorption/precipitation. J Hazard Mater 201:60–67

U.S. EPA (1985) Health and Environmental Effects Profile for Aniline. U.S. Environmental Protection Agency, Office of Solid Waste and Emergency Response Washington, D.C., Environmental Criteria and Assessment Office, Cincinnati, OH. ECAO-CIN-P136

Ullhyan A, Ghosh UK (2012) Biodegradation of phenol with immobilized *Pseuodomonas putida* activated carbon packed bio-filter tower. Afr J Biotechnol 11(85):15160–15167

Vernon JD, Bonzongo JCJ (2014) Volatilization and sorption of dissolved mercury by metallic iron of different particle sizes: implications for treatment of mercury contaminated water effluents. J Hazard Mater 276:408–414

Wasi S, Tabrez S, Ahmad M (2013) Use of *Pseudomonas* spp. for the bioremediation of environmental pollutants: a review. Environ Monit Assess 185(10):8147–8155

Yaacob WZW, Kamaruzaman N, Rahim A (2012) Development of nano-zero valent iron for the remediation of contaminated water. Chem Eng 28:25–30

Yang K, Wu W, Jing Q, Zhu L (2008) Aqueous adsorption of aniline, phenol, and their substitutes by multi-walled carbon nanotubes. Environ Sci Technol 42(21):7931–7936

Yang Y, Guo J, Hu Z (2013) Impact of nano zero valent iron (NZVI) on methanogenic activity and population dynamics in anaerobic digestion. Water Res 47(17):6790–6800

Yuan C, Lien HL (2006) Removal of arsenate from aqueous solution using nanoscale iron particles. Water Qual Res J Can 41:210–215

Zhang WX (2003) Nanoscale iron particles for environmental remediation: an overview. J Nanopart Res 5(3–4):323–332

Zhao et al. (2011) United States patent. Patent no.: 7,887,880 B2. Date of patent: Feb 15

Zissi U, Lyberatos G, Pavlou S (1997) Biodegradation of p-aminoazobenzene by *Bacillus subtilis* under aerobic conditions. J Ind Microbiol Biotechnol 19(1):49–55